



A single-step competitive binding assay for mapping of single DNA molecules

Lena K. Nyberg^{a,1}, Fredrik Persson^{b,c,1}, Johan Berg^a, Johanna Bergström^a, Emelie Fransson^a, Linnea Olsson^a, Moa Persson^a, Antti Stålnacke^a, Jens Wigenius^a, Jonas O. Tegenfeldt^{c,d}, Fredrik Westerlund^{a,*}

^a Department of Chemical and Biological Engineering, Chalmers University of Technology, Gothenburg, Sweden

^b Department for Cell and Molecular Biology, Uppsala University, Uppsala, Sweden

^c Department of Physics, University of Gothenburg, Gothenburg, Sweden

^d Department of Physics, Lund University, Lund, Sweden

ARTICLE INFO

Article history:

Received 18 November 2011

Available online 7 December 2011

Keywords:

DNA mapping
Nanofluidic channels
Competitive assay
Single DNA molecules
Fluorescence microscopy

ABSTRACT

Optical mapping of genomic DNA is of relevance for a plethora of applications such as scaffolding for sequencing and detection of structural variations as well as identification of pathogens like bacteria and viruses. For future clinical applications it is desirable to have a fast and robust mapping method based on as few steps as possible. We here demonstrate a *single-step* method to obtain a DNA barcode that is directly visualized using nanofluidic devices and fluorescence microscopy. Using a mixture of YOYO-1, a bright DNA dye, and netropsin, a natural antibiotic with very high AT specificity, we obtain a DNA map with a fluorescence intensity profile along the DNA that reflects the underlying sequence. The netropsin binds to AT-tetrads and blocks these binding sites from YOYO-1 binding which results in lower fluorescence intensity from AT-rich regions of the DNA. We thus obtain a DNA barcode that is dark in AT-rich regions and bright in GC-rich regions with kilobasepair resolution. We demonstrate the versatility of the method by obtaining a barcode on DNA from the phage T4 that captures its circular permutation and agrees well with its known sequence.

© 2011 Elsevier Inc. All rights reserved.

1. Introduction

While base-by-base sequencing provides genomic information with the ultimate resolution of single nucleotides it suffers from several limitations. Traditional Sanger shotgun sequencing protocols, as well as its more cost- and time-effective followers, are all based on fragmenting the unknown DNA and sequencing each fragment independently [1]. The results from each fragment are subsequently pieced together using powerful bioinformatics algorithms. However, long-range information is lost in the process and repeated regions are notoriously difficult to sequence reliably.

Optical mapping techniques on the other hand are based on direct imaging of intact single DNA molecules where the internal order is preserved, however at the price of a reduced resolution set by the optical system and the packing density of the DNA. Applications include mapping of structural variations, scaffolding for sequencing and identification of pathogens like viruses and bacteria. The earliest forms of mapping were banding of condensed chromosomes giving a resolution on the order of 1–10 Mb. Mapping based on fluorescence *in situ* hybridization (FISH) gives more

specific information but with similar resolution [2]. On the other hand, stretching the DNA on surfaces [3–5] or in nanochannels [6] and visualizing it using fluorescence microscopy has attracted significant attention with its relative ease of use and higher resolution. Using standard fluorescence microscopy techniques, where DNA is stretched in nanochannels or on glass, a resolution of 1 kbp is obtainable.

There is a fair range of optical methods, mainly based on fluorescence microscopy, for large-scale genome mapping on the single DNA molecule level [7–10]. Early methods include DNA immobilization on patterned surfaces, fluorescent labeling, and cutting with restriction enzymes, in order to detect the specific sites the enzyme recognizes and thereby create a map of the DNA [10]. Similar approaches, using nicking enzymes, where the DNA remains in one piece have also been demonstrated [8]. More recently, Neely et al. demonstrated how methyltransferases can be used to attach fluorophores to specific 6-base sequences on DNA [11]. Using several different methyltransferases a multi-color high-resolution mapping can be obtained in an efficient way.

Using nanofluidic channels to linearize long DNA molecules, rather than stretching them on glass slides, has the benefit of ensuring reproducibility. When a large piece of DNA is introduced into a nanochannel, the confinement will lead to spontaneous

* Corresponding author. Fax: +46 31 772 3858.

E-mail address: fredrik.westerlund@chalmers.se (F. Westerlund).

¹ The two authors contributed equally.

stretching of the DNA along the channel, with an extension that scales linearly with contour length. The DNA is thus held in place without the need of any external stretching forces, so that DNA of arbitrary length can be analyzed. Previously, Reisner et al. have demonstrated the use of nanofluidic channels in combination with local DNA melting to obtain a DNA barcode [12]. By using a DNA dye that has a much brighter fluorescence when bound to double stranded DNA than to single stranded they obtained a fluorescence intensity profile along the DNA that reflects the underlying AT/GC ratio. In order to detect melting at an experimentally convenient temperature a denaturant, formamide, is added to decrease the strength of the hydrogen bonds. While melting mapping is capable of producing high-quality barcodes, there are two important experimental difficulties that may deter a wider audience. Firstly, it requires a detailed control of the temperature in the nanochannels, which is experimentally tricky and in turn makes the setup more complicated. Secondly, it requires a noxious chemical, formamide, which acts as a denaturant. Formamide also hampers the imaging conditions in the microscope by reducing the fluorescence intensity of the dye. An optimal future mapping method based on the same simple underlying principle – a barcode based on differences in fluorescence intensity between AT-rich and GC-rich regions – would thus be one where the pattern is formed *outside* the chip, and where the measurements can be performed at equilibrium and at ambient temperature without the use of any toxic reagents. For simplicity and ease of use it would be desirable that the sample preparation can be done in a *single step*.

An alternative mapping assay that fulfills these criteria would be to use DNA-binding molecules with different sequence specificities and dissimilar fluorescent properties. One possible approach would be to use sequence specific fluorescent dyes. However, existing dyes typically have insufficient sequence specificity or too weak fluorescence for detection in a standard fluorescence microscope. Instead, we combine a non-fluorescent molecule with exceptional sequence specificity with a commonly used fluorescent DNA dye.

We here demonstrate an assay that can be used to obtain barcodes in a simple *single-step* procedure by adding a mixture of netropsin, a natural antibiotic with a very high specificity for AT-rich sequences [13,14] and the bis-intercalating dye YOYO-1 to a long piece of DNA that is stretched in a nanofluidic channel. The result is a reproducible fluorescence intensity profile along the DNA that reflects the underlying AT/GC content on the single DNA molecule level.

2. Materials and methods

2.1. Chemicals

The TBE buffer was purchased from Medicago as 10× TBE tablets and dissolved in milli-Q water to the desired concentration. β-Mercaptoethanol (Sigma–Aldrich) was added to the buffer (3% v/v) to suppress photoniccking of the DNA. Netropsin was purchased from Sigma–Aldrich and YOYO-1 was purchased from Invitrogen and subsequently added at the desired concentrations by dilution in buffer. Throughout the study the term “excess” relates to the ratio between the concentrations of netropsin and YOYO-1. DNA from phage lambda (λ-DNA, 48.5 kbp) was purchased from New England Biolabs and T4GT7 DNA (T4-DNA, 166.5 kbp) provided by Nippon Gene and purchased through Wako.

2.2. Stretching DNA on glass slides

For stretching on glass slides, λ-DNA was stained with YOYO-1 (one dye per 10 basepairs) and heated for 3 h at 50 °C. Netropsin

was subsequently added and the DNA was stretched on positively charged glass slides obtained from Thermo Scientific (Menzel-Gläser). The experiments were performed in 2× TBE buffer with λ-DNA stained with YOYO-1 (one dye per 10 basepairs) at 8000 times excess of netropsin (in relation to YOYO-1).

2.3. Stretching DNA in nanofluidic chips

The nanofluidic chips were fabricated in fused silica using methods described elsewhere [6]. The channels were approximately $100 \times 150 \text{ nm}^2$ in cross-section and 500 μm long. The different DNAs were either prestained with YOYO-1 (one dye per 10 basepairs) after which netropsin was added, or netropsin and YOYO-1 were premixed and added to the DNA. The experiments were performed in 0.5× TBE buffer.

The DNA is loaded into one of the microchannels of the chip and transferred to the nanochannel array by an applied pressure difference. By applying pressure over two connected microchannels the DNA is subsequently injected into the nanochannels.

The microscope used is a Zeiss Axiovision equipped with a Photometrics Evolve EMCCD camera and a 100× oil immersion objective (NA = 1.46) from Zeiss.

Image stacks with 100 images were recorded for each molecule with an exposure time of 100 ms per image at 10 frames per second.

2.4. Analysis

Data analysis was performed with the freeware ImageJ (<http://rsbweb.nih.gov/ij/>) and a custom-written MatLab based software. For the studies on glass slides the traces were obtained from a single image and a profile plot was obtained using ImageJ. For DNA confined in nanochannels a kymograph (timetrace) was extracted for each movie using ImageJ and aligned using the MatLab software. The initial alignment is done on the center of the molecule to eliminate the effects of drift along the nanochannel. The intensity profile from the molecule is fitted to a linear combination of error functions, an extension of the procedure used in Ref. [15].

A finer alignment procedure is subsequently performed on distinct features (peaks or dips in intensity) along the DNA. This alignment step is commonly performed in multiple steps where the initial steps are performed on a Gaussian or average smoothed kymograph to suppress the effects from noise. This alignment step is based on finding local maxima/minima in the profile for each frame and then match the closest features between neighboring frames. The result is then verified by manual inspection. The actual alignment between two features is done by linearly extracting/compressing the profile between the adjacent tracked features for all frames to match the average distance between the features in all frames (lines in the kymograph).

2.5. Theoretical barcodes

The theoretical barcodes for λ-DNA and T4GT7-DNA were calculated by first running a moving average with a window size of five nucleotides over the whole sequence (Accession Nos. NC001416 for λ-DNA and NC000866 for T4 DNA and taking into account that nucleotides number 165,255–168,510 are lacking in T4GT7) to obtain a measure for the relative binding affinity of the ligand which binds to four consecutive basepairs in the minor groove. To make a direct comparison between the theoretical barcodes and the experimental data possible, the resolution of the experimental microscope setup is accounted for in the theoretical map by convolution with the point-spread function (PSF) of the microscope. The PSF was estimated by fitting a Gaussian profile to the intensity profile of a quantum dot imaged using the same microscope. A standard deviation of approximately 0.3 μm was obtained.

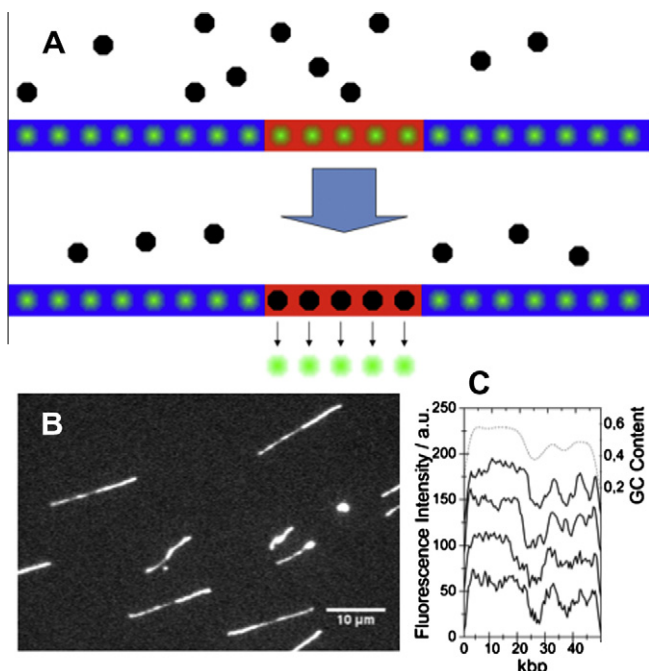


Fig. 1. (A) Schematic demonstrating the two-step competitive binding assay. A sequence selective molecule (black) is added to DNA homogenously labeled with a fluorescent dye (green). The DNA contains two regions of mixed sequence (blue) and one region with a high AT content (red). If the candidate molecule is AT selective (as suggested from the image), it will specifically replace the dye in the red region thereby locally decreasing the fluorescence intensity. (B) λ -DNA stained with YOYO-1 (one dye per 10 basepairs) where an 8000-fold excess (relative to YOYO-1) has been added. The DNA is stretched on positively charged glass. (C) Fluorescence intensities along the contour for the four fully stretched λ -DNA molecules shown to the left (solid lines) together with the local GC content of λ -DNA based on its known sequence (dashed line), calculated as described in Section 2. The traces are shifted vertically for clarity. The left y-axis corresponds to the experimental data and the right y-axis corresponds to the known sequence. (For interpretation of the references to color in this figure legend, the reader is referred to the web version of this paper.)

This corresponds to approximately 1800 basepairs since the DNA is stretched to approximately 50% of its contour length in the nano-channels used here. A corresponding Gaussian filter convoluted with the theoretical barcode yields the final profiles shown as dashed lines in Figs. 1C and 4B, D.

3. Results and discussion

A schematic of our proof-of-principle experiment is shown in Fig. 1A. By adding a molecule with a high AT selectivity to DNA that

is prestained with a fluorescent dye, we kick out the fluorescent dye from AT-rich regions. This results in a fluorescence intensity variation along the DNA that reflects the underlying AT/GC content; bright regions are GC-rich while dark regions are AT-rich. Netropsin is a commercially available, naturally occurring antibiotic with a large selectivity for AT-rich sequences [13,14] and is therefore an excellent candidate to use together with the common DNA dye YOYO-1.

We added 8000-fold excess of netropsin to YOYO-1-labeled (one dye per ten basepairs) lambda phage DNA (λ -DNA) molecules and stretched them on a positively charged glass slide (Fig. 1B). The need for a large excess of netropsin is due to the significant difference in binding constants of the two molecules. Intercalators, such as YOYO-1, generally have a high DNA binding affinity while minor-groove binders generally have a lower binding affinity but a much greater sequence selectivity. The binding constant of YOYO-1 is greater than 10^{10} M^{-1} [16–18], while netropsin has a binding constant of approximately 10^8 M^{-1} to poly(dAdT)₂ and much lower for mixed sequences [13,14]. The fluorescence intensity varies in a very consistent manner along each of the four different DNA molecules, one of the halves of the DNA is much brighter and has less variations in intensity than the other half. Fig. 1C shows the fluorescence intensity profiles along the molecules in Fig. 1B. It is evident from these plots that the resulting fluorescence intensity pattern reflects the known local GC fraction of the λ -DNA well with a dark dip in intensity in the center of the sequence and a satellite dip on one of the sides.

To ensure a reliable and reproducible stretching of the DNA we turned to nanofluidic channels and stretched the DNA by confinement [15]. Fig. 2 shows representative λ -DNA molecules, prestained with YOYO-1, at increasing excess concentrations of netropsin. As the netropsin concentration increases we see that the dark features on the DNA become increasingly prominent. It is interesting to note that the fluorescence intensity from some regions *increases* as we add up to approximately 2000- to 4000-fold excess netropsin. This is because when netropsin replaces YOYO-1 in the AT-rich regions, the YOYO-1 can rebind in other regions with lower netropsin coverage, since the DNA is not fully saturated with YOYO-1 at the dye concentrations used. The fact that the length of the DNA does not change up to 2000-fold excess netropsin indicates that there is no significant decrease in the overall amount of YOYO-1 bound, since YOYO-1 contributes to the contour length due to its intercalative binding mode while the groove bound netropsin does not [19]. As expected, at higher excess of netropsin the contour length of the DNA decreases and at the same time the overall fluorescence intensity decreases as netropsin blocks more and more YOYO-1 binding sites. The fluorescence intensity along the DNA molecules at each netropsin concentration is shown in Fig. 2 (bottom). For increasing netropsin concentrations the central dark AT-rich region is

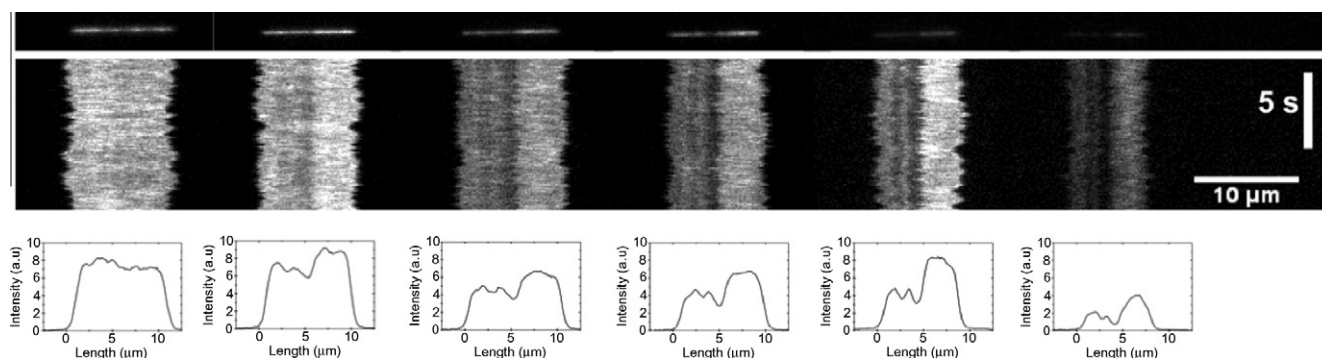


Fig. 2. (Top) Single image of a DNA molecule. (Center) Kymographs of λ -DNA stained with YOYO-1 at varying netropsin excess. (Bottom) Average fluorescence intensity along each DNA molecule. Note that there exists an optimum netropsin concentration for which the contrast is at a maximum. The netropsin excess increases from left to right and is 0, 500, 1000, 2000, 4000 and 8000, respectively.

increasingly prominent and the appearance of another dark region next to it, also seen in the theoretical barcode (see Fig. 1C) is evident. We can thus obtain complementary information by varying the netropsin concentration. It is however worth to notice that the change in fluorescence intensity pattern varies only slightly with concentration, making our assay so robust that small fluctuations in concentrations will not significantly change the information obtained.

λ -DNA is an excellent model system to demonstrate the proof-of-principle of the assay due to its very large variation in AT content along its contour. We would however like to challenge our assay by studying a DNA with a more even local sequence distribution. We would also, for future clinical applications, like to have a simple kit, with a mixture of netropsin and YOYO-1, that creates the map of the DNA in a *single* step in the test tube (schematically shown in Fig. 3A). We therefore add the mixture of YOYO-1 and netropsin (1:2000) to T4GT7 DNA (T4-DNA) to a concentration of one YOYO-1 per five basepairs and stretched it in nanofluidic channels. We observe, already in a single image of a T4-DNA molecule, that the two halves of the T4-DNA molecule have different fluorescence intensities, suggesting that they have different AT/GC content, and we also observe local variations in intensity (Fig. 3B).

Fig. 3C compares kymographs of four different representative T4-DNA molecules where the mixture has been added (recorded

on two different sample preparations). The DNA molecules fluctuate and diffuse in the channels, which leads to distortions in the obtained barcode, decreasing the resolution. We therefore align the kymographs, first based on the center of mass and subsequently on distinct features in the barcode pattern, in order to compensate for such fluctuations (see Section 2 for details). The obtained straightened kymographs, with distinct barcodes, are the ones shown in Fig. 3C. At a first glance, the fluorescence intensity variations along the molecules do not appear to resemble each other at all. We identify however two bright patches that seem to be at the same distance from each other in all four molecules. It is

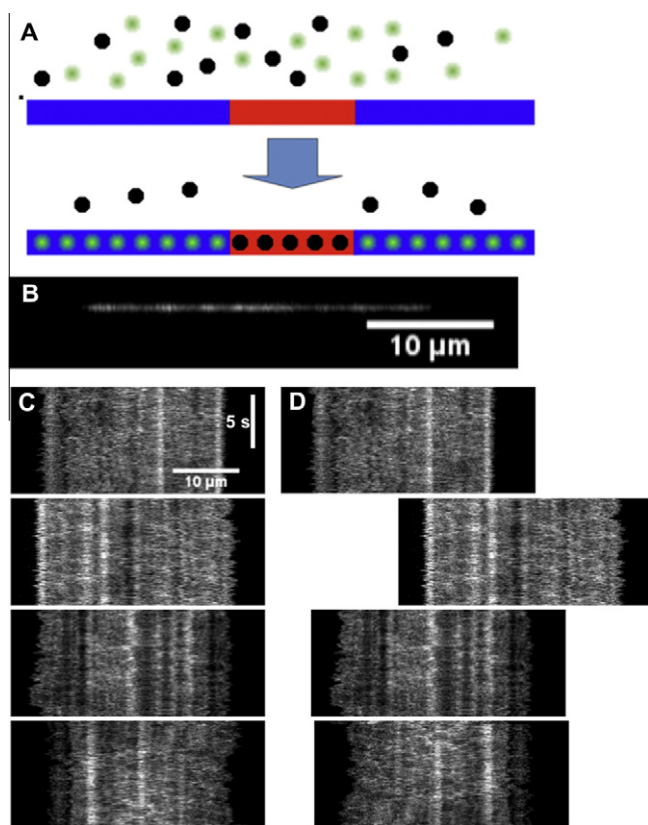


Fig. 3. (A) Schematic demonstrating a single-step competitive binding assay. The sequence selective molecule (black) and the fluorescent dye (green) are premixed and added simultaneously to DNA. The DNA contains two regions of mixed sequence (blue) and one region with a high AT content (red). If the candidate molecule is AT selective (as suggested from the image), it will specifically bind in the red region thereby preventing the dye to bind, which leads to a lower fluorescence intensity. (B) T4-DNA molecule stretched in a nanofluidic channel where a 1:2000 mixture of YOYO-1 (one YOYO per five basepairs) and netropsin has been added outside the chip. (C) Aligned kymographs for four representative T4-DNA molecules recorded on two different occasions. (D) The traces in B aligned by eye to visualize the circular permutation of T4-DNA. (For interpretation of the references to color in this figure legend, the reader is referred to the web version of this paper.)

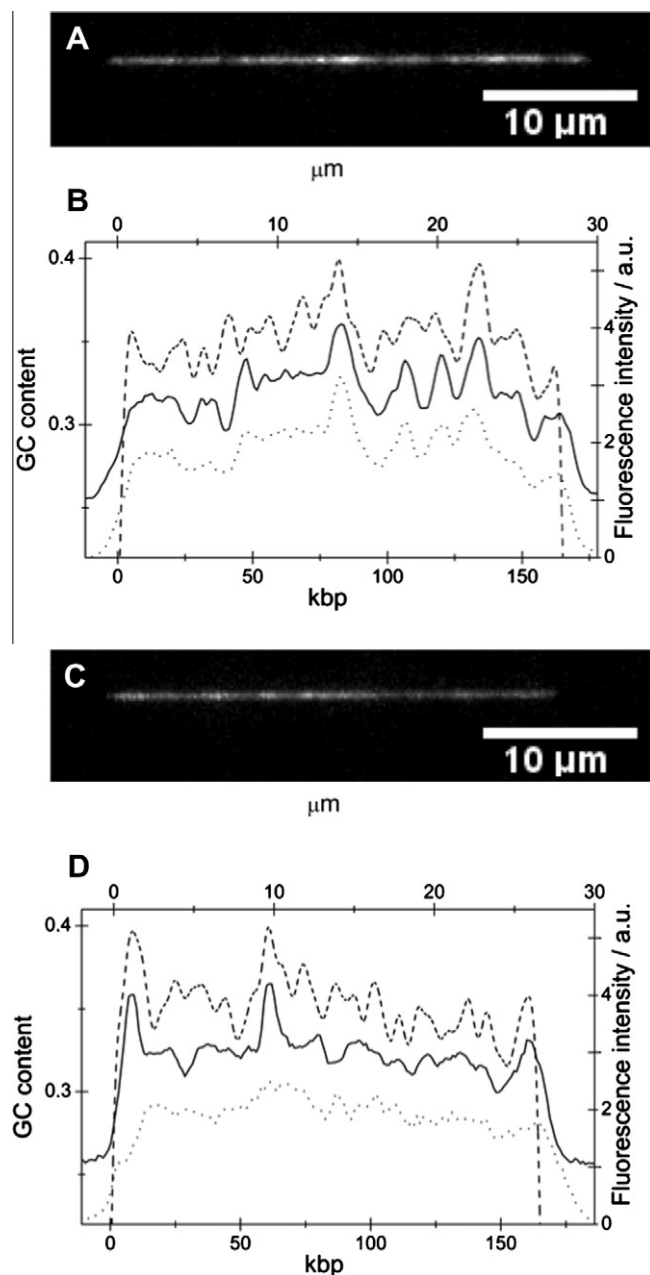


Fig. 4. Traces of the fluorescence intensity for raw-data kymographs (dotted lines), traces of the fluorescence intensity for the aligned kymographs (solid lines) as well as the theoretical barcode pattern for T4-DNA (dashed lines) for two representative T4-DNA molecules shown in A and C. The theoretical barcode pattern has been matched to the obtained fluorescence intensity traces from the aligned kymographs by eye. The aligned traces are shifted vertically for clarity. The theoretical curves are calculated as described in Section 2. The left y-axis is based on the known sequence and the right y-axis corresponds to the experimental data.

known from the literature that the T4-DNA genome is circularly permuted [20], meaning that each linearized T4-DNA molecule will start and end at a different sequence. Furthermore the DNA can enter the nanochannel with either end first. With this in mind we can manually align the four kymographs relative to each other. Using the two most distinct bright features in each kymograph we can position the molecules relative to each other (Fig. 3D) and then observe several other distinct features that are common for all of the four molecules, justifying the alignment.

In order to be useful, the assay not only has to yield a reproducible variation in intensity along the sequence, the obtained barcode should also reflect the genetic sequence of the molecule in a predictable way. Fig. 4 compares experimentally obtained intensity traces for two T4-molecules with the known local GC-content of T4-DNA, compensated for the characteristics of the experimental setup (see Section 2 for details on how the theoretical trace was calculated). We are, for both molecules, able to identify the main features of the T4 barcode using our method. The two most intense bright features, and the distance between them, are perfectly captured with our assay, along with several weaker features. Fig. 4 also stresses the importance of the aligning process in order to improve the quality of the obtained barcode. Many of the distinct features are blurred by thermal fluctuations and diffusion but by aligning the kymographs we are able to increase the quality of the obtained barcode significantly.

Comparing our method to existing barcoding techniques we note that our labeling protocol works in a single step, that the barcode is formed already in the test tube and that we, along with the DNA of interest, only use commercially available molecules. The use of nanofluidics ensures high-throughput, a relaxed DNA in its equilibrium conformation and the possibility to average over long times to improve the signal-to-noise. In particular, comparing with the melting mapping assay, we note that the measurements are done at equilibrium, at ambient temperature, that the measurements can be done without significant amounts of noxious chemicals and that the contrast of the barcode pattern is only weakly dependent on the time the DNA spends in the nanochannels. The assay is applicable in several different fields of single-molecule genomic DNA analysis and the required resolution of the obtained map, both in AT/GC content as well as on the number of basepairs, depends strongly on the specific application. We note that the degree of stretching, and thus the resolution based on the number of base-pairs, can easily be tuned in our nanofluidic setup. We also note that our method, along with other barcoding techniques works on intact single DNA molecules without the need for DNA amplification or cell-growth.

To conclude, we have demonstrated a *single-step* method to map DNA on the single molecule level with on the order of kilobasepair resolution. By adding netropsin, a drug with an extreme preference for AT basepairs, and YOYO-1, a fluorescent dye with no sequence selectivity we obtain intensity maps that reflect the underlying AT/GC ratio. We apply our assay to T4-DNA and successfully aligned circularly permuted individual molecules based on their barcodes, despite the relatively uniform local AT/GC ratio along the molecule that makes it difficult to create a high-contrast pattern. We also show that we can tune the level of information obtained by varying the netropsin concentration. We envision

the application of our simple assay in a variety of fields, such as identification of microorganism, scaffolding for base-by-base sequencing and detection of structural variations.

Acknowledgments

This project is funded by the Chalmers Area of Advance in Nanoscience and Nanotechnology and the Swedish Foundation for Strategic Research. J.O.T. acknowledges support from the Swedish Research council Grants No. 2007-584 and 2007-4454 and the European Union 7th Framework Programme (7RP/2007-2013) under Grant agreement No. 201418 (READNA).

References

- [1] J. Shendure, H. Ji, Next-generation DNA sequencing, *Nat. Biotechnol.* 26 (10) (2008) 1135–1145.
- [2] O.J. Miller, E. Therman, *Human Chromosomes*, Springer-Verlag, New York, PA, 2001.
- [3] D. Bensimon, A.J. Simon, V. Croquette, A. Bensimon, et al., Stretching DNA with a receding meniscus – experiments and models, *Phys. Rev. Lett.* 74 (23) (1995) 4754–4757.
- [4] A. Bensimon, A.J. Simon, A. Chiffaudel, et al., Alignment and sensitive detection of DNA by a moving interface, *Science* 265 (5181) (1994) 2096–2098.
- [5] D.C. Schwartz, X. Li, L.I. Hernandez, et al., Ordered restriction maps of *Saccharomyces cerevisiae* chromosomes constructed by optical mapping, *Science* 262 (5130) (1993) 110–114.
- [6] F. Persson, J.O. Tegenfeldt, DNA in nanochannels – directly visualizing genomic information, *Chem. Soc. Rev.* 39 (3) (2010) 985–999.
- [7] R.K. Neely, J. Deen, J. Hofkens, Optical mapping of DNA: single-molecule-based methods for mapping genomes, *Biopolymers* 95 (5) (2011) 298–311.
- [8] S.K. Das, M.D. Austin, M.C. Akana, Single molecule linear analysis of DNA in nano-channel labeled with sequence specific fluorescent probes, *Nucleic Acids Res.* 38 (18) (2010).
- [9] E.Y. Chan, N.M. Goncalves, R.A. Hausler, et al., DNA mapping using microfluidic stretching and single-molecule detection of fluorescent site-specific tags, *Genome Res.* 14 (2004) 1137–1146.
- [10] W. Cai, J. Jing, B. Irvin, et al., High-resolution restriction maps of bacterial artificial chromosomes constructed by optical mapping, *Proc. Natl. Acad. Sci. USA* 95 (7) (1998) 3390–3395.
- [11] R.K. Neely, P. Dedeker, J. Hotta, et al., DNA fluorocode: a single molecule, optical map of DNA with nanometre resolution, *Chem. Sci.* 1 (4) (2010) 453–460.
- [12] W. Reisner, N.B. Larsen, A. Silahatoglu, et al., Single-molecule denaturation mapping of DNA in nanofluidic channels, *Proc. Natl. Acad. Sci. USA* 107 (30) (2010) 13294–13299.
- [13] C. Zimmer, C. Mark, C. Schnider, W. Guschlbauer, Influence of nucleotide-sequence on dA.dT-specific binding of netropsin to double stranded DNA, *Nucleic Acids Res.* 6 (8) (1979) 2831–2837.
- [14] M.W. Van Dyke, R.P. Hertzberg, P.B. Dervan, Map of distamycin, netropsin, and actinomycin binding sites on heterogeneous DNA: DNA cleavage-inhibition patterns with methidiumpropyl-EDTA-Fe(II), *Proc. Natl. Acad. Sci. USA* 79 (18) (1982) 5470–5474.
- [15] J.O. Tegenfeldt, C. Prinz, H. Cao, et al., The dynamics of genomic-length DNA molecules in 100-nm channels, *Proc. Natl. Acad. Sci. USA* 101 (30) (2004) 10979–10983.
- [16] A. Larsson, C. Carlsson, M. Jonsson, B. Albinsson, Characterization of the binding of the fluorescent dyes YO and YOYO to DNA by polarized-light spectroscopy, *J. Am. Chem. Soc.* 116 (19) (1994) 8459–8465.
- [17] A.N. Glazer, H.S. Rye, Stable dye-DNA intercalation complexes as reagents for high-sensitivity fluorescence detection, *Nature* 359 (6398) (1992) 859–861.
- [18] H.S. Rye, S. Yue, D.E. Wemmer, et al., Stable fluorescent complexes of double-stranded DNA with bis-intercalating asymmetric cyanine dyes – properties and applications, *Nucleic Acids Res.* 20 (11) (1992) 2803–2812.
- [19] M.L. Kopka, C. Yoon, D. Goodsell, et al., The molecular origin of DNA-drug specificity in netropsin and distamycin, *Proc. Natl. Acad. Sci. USA* 82 (5) (1985) 1376–1380.
- [20] G. Streisinger, R.S. Edgar, G.H. Denhardt, Chromosome structure in phage T4, I. Circularity of linkage map, *Proc. Natl. Acad. Sci. USA* 51 (5) (1964) 775–779.